Int. J. Heat Mass Transfer. Vol. 21, pp. 701–708

0017-9310/78/0601-0701 $02.00/0

FULLY DEVELOPED NATURAL COUNTERFLOW IN A LONG HORIZONTAL PIPE WITH DIFFERENT END TEMPERATURES

A. BEJAN and C. L. TIEN
Department of Mechanical Engineering, University of California, Berkeley, CA, U.S.A.

(*Received* 22 *July* 1977 *and in revised form* 21 *October* 1977)

Abstract—The temperature difference applied across the two ends of a horizontal duct generates a natural counterflow in which colder fluid flows along the bottom of the duct towards the warm end while a warmer stream flows in the opposite direction along the top. The paper presents an asymptotic solution for the velocity and temperature distributions in the middle portion of a long horizontal pipe with conducting wall. The influence of circumferential heat conduction through the pipe wall on the temperature distribution in the fluid has been investigated. An analytical expression has been established for the net axial heat-transfer rate by counterflow natural convection. The present results for the temperature distribution in the pipe wall are compared with numerical results reported recently.

NOMENCLATURE

a_1, a_2, constants, equation (24);
C, wall thermal resistance parameter, equation (12);
g, gravitational acceleration [m/s^2];
k, fluid thermal conductivity [W/mK];
k_w, wall thermal conductivity [W/mK];
K_1, K_2, constants of core solution, equation (18);
L, pipe length [m];
Nu, Nusselt number, equation (33);
Pr, Prandtl number ν/α;
P, dimensionless pressure, equation (6b);
P^*, pressure [N/m^2];
Q, convective heat leak [W];
r, dimensionless radial position, equation (4a);
r^*, radial position [m];
r_0, radius [m];
Ra, Rayleigh number, equation (7);
t, wall thickness [m];
T, dimensionless temperature, equation (6a);
T^*, temperature [K];
T_1, cold end temperature [K];
T_2, warm end temperature [K];
u, dimensionless radial velocity, equation (5a);
u^*, radial velocity [m/s];
v, dimensionless circumferential velocity, equation (5b);
v^*, circumferential velocity [m/s];
w, dimensionless axial velocity, equation (5c);
w^*, axial velocity [m/s];
z, dimensionless axial position, equation (4b);
z^*, axial position [m].

Greek symbols

α, fluid thermal diffusivity [m^2/s];
β, coefficient of volumetric thermal expansion [K^{-1}];
θ, angular position, Fig. 1;
ν, kinematic viscosity [m^2/s];
ρ, density [kg/m^3];
ϕ, dimensionless wall temperature function, equation (36);
ψ, function, equation (24);
Ψ_{II}, second order stream function, Fig. 4.

Subscripts

0,I,II, zeroth, first, second order approximations.

1. INTRODUCTION

THE TEMPERATURE difference applied across the ends of a horizontal pipe filled with stagnant fluid gives rise to a counterflow natural convection pattern of the kind sketched in Fig. 1. The fluid motion is caused by the axial density variation associated with the axial temperature gradient. The resulting changes in the hydrostatic pressure gradient forces the cold fluid to flow along the bottom towards the warm end while the warmer stream returns along the top half of the pipe.

In spite of its common existence and relatively simple configuration, this type of flow has received relatively little attention. Quite recently, Hong [1] studied the effect of this flow on the temperature distribution in the conduit wall. His main objective was to predict the circumferential wall temperature gradient which is important in thermal stress analysis. His numerical solution, however, is based on a simulated forced-convection system in which there is a solid wall across the horizontal centerplane and the warm and cold streams flow in opposite directions in two semi-circular tubes. The only other effort of analyzing a related flow is also recent. In a sequence of four articles, Cormack, Leal, Imberger, Seinfeld and Stone [2–5] studied the natural counterflow in a horizontal parallel-plate channel with closed ends. Their work was inspired by the interest in the spreading of thermal pollution by natural convection in shallow bodies of water. Bejan and Tien [6] have recently completed a study of the free convection heat transport through

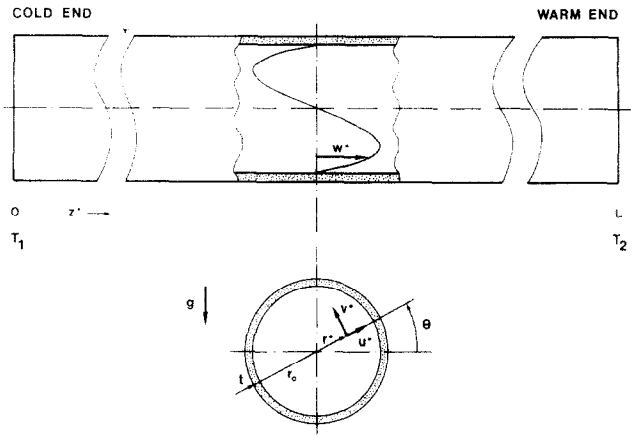

FIG. 1. Natural counterflow in a long horizontal pipe with ends maintained at different temperatures.

parallel-plate horizontal channels with either one end or both ends open. The work was motivated by the need to evaluate heat-transfer rates through horizontal channels filled with liquid helium. Channels of this type constitute a basic thermal design feature in large superconducting winding systems [7].

The present article constitutes an analytical study of the velocity and temperature fields in the horizontal counterflow natural convection inside a long pipe with the final objective of estimating the convection heat leak carried by the two streams from the warm end to the cold end. The pipe wall is modeled as a conducting sheet, insulated with respect to the ambient (i.e. the heat loss from the pipe to the ambient is assumed negligible). The paper presents an asymptotic solution for the velocity and temperature field valid in the limit when the pipe is long ($r_0/L \to 0$) or the Rayleigh number based on end-to-end temperature difference approaches zero.

In the next section, we begin with defining the heat-transfer problem as described in Fig. 1. In Section 3 we present analytical expressions for the velocity and temperature distributions inside the middle portion of the long horizontal pipe. Based on this analysis, in Section 4 we present the Nusselt number for axial heat transfer, as a function of the Rayleigh number, the ratio of pipe length to radius and the wall circumferential thermal conductance. In Section 5 we calculate the temperature distribution around the pipe wall, information required by thermal stress analysis. Finally, in Section 6 we compare our analytical expression for the temperature distribution in the pipe wall with the numerical results reported by Hong [1].

2. PROBLEM STATEMENT

Consider the horizontal pipe of Fig. 1. The pipe radius r_0 is much larger than the wall thickness t and the pipe length L is much larger than r_0. Assuming the fluid is incompressible, the steady state equations governing the conservation of mass, momentum and energy in fluid are, respectively,

$$\frac{u}{r}+\frac{\partial u}{\partial r}+\frac{1}{r}\frac{\partial v}{\partial \theta}+\frac{\partial w}{\partial z}=0 \tag{1}$$

$$\frac{1}{Pr}\left(u\frac{\partial u}{\partial r}+\frac{v}{r}\frac{\partial u}{\partial \theta}+w\frac{\partial u}{\partial z}-\frac{v^2}{r}\right) = -\frac{gr_0^3}{\alpha\nu}\sin\theta+Ra(\sin\theta)T - \frac{\partial P}{\partial r}+\nabla^2 u-\frac{u}{r^2}-\frac{2}{r^2}\frac{\partial v}{\partial \theta} \tag{2a}$$

$$\frac{1}{Pr}\left(u\frac{\partial v}{\partial r}+\frac{v}{r}\frac{\partial v}{\partial \theta}+w\frac{\partial v}{\partial z}+\frac{uv}{r}\right) = -\frac{gr_0^3}{\alpha\nu}\cos\theta+Ra(\cos\theta)T - \frac{1}{r}\frac{\partial P}{\partial \theta}+\nabla^2 v+\frac{2}{r^2}\frac{\partial u}{\partial \theta}-\frac{v}{r^2} \tag{2b}$$

$$\frac{1}{Pr}\left(u\frac{\partial w}{\partial r}+\frac{v}{r}\frac{\partial w}{\partial \theta}+w\frac{\partial w}{\partial z}\right)=-\frac{\partial P}{\partial z}+\nabla^2 w \tag{2c}$$

$$u\frac{\partial T}{\partial r}+\frac{v}{r}\frac{\partial T}{\partial \theta}+w\frac{\partial T}{\partial z}=\nabla^2 T. \tag{3}$$

The system coordinates r, θ, z and the velocity components u, v, w are clearly indicated in Fig. 1, and T and P stand for fluid temperature and pressure, respectively. Equations (1)–(3) have already been non-dimensionalized by having introduced the following dimensionless variables

$$r=r^*/r_0, \quad z=z^*/r_0 \tag{4a,b}$$

$$u=u^*r_0/\alpha, \quad v=v^*r_0/\alpha, \quad w=w^*r_0/\alpha \tag{5a,b,c}$$

$$T=\frac{T^*-T_1}{T_2-T_1}, \quad P=\frac{P^*r_0^2}{\rho\alpha\nu}. \tag{6a,b}$$

The quantities denoted by an asterisk represent the dimensional variables of the problem. These, as well as the other symbols appearing in equations (4)–(6), are defined in the nomenclature.

In equations (1)–(3), Pr is the Prandtl number ν/α, Ra is the Rayleigh number based on the pipe radius,

$$Ra=\frac{g\beta r_0^3(T_2-T_1)}{\alpha\nu} \tag{7}$$

and ∇^2 is the Laplacian operator in cylindrical coordinates,

$$\nabla^2=\frac{\partial^2}{\partial r^2}+\frac{1}{r}\frac{\partial}{\partial r}+\frac{1}{r^2}\frac{\partial^2}{\partial \theta^2}+\frac{\partial^2}{\partial z^2}. \tag{8}$$

In stating the governing equation we made use of the Boussinesq approximation,

$$\rho = \rho_0[1-\beta(T^*-T_0)]. \tag{9}$$

where subscript 0 represents properties of a reference state.

The problem consists of determining the velocity field u, v, w, and the temperature field T as a function of r, θ, z, subject to equations (1)–(3) and the following boundary conditions. First, the no-slip condition at the wall requires

$$u = v = w = 0 \quad \text{at} \quad r = 1. \tag{10}$$

The temperature boundary condition at $r = 1$ is tied to the presence of heat conduction in the pipe wall. Since $t \ll r_0$, we may treat the pipe wall as a conducting sheet of zero thickness. The temperature distribution over this surface is dictated by the heat conduction equation,

$$\frac{\partial^2 T}{\partial z^2} + \frac{1}{r^2}\frac{\partial^2 T}{\partial \theta^2} = C\frac{\partial T}{\partial r}, \quad r = 1, \tag{11}$$

where C is a measure of the wall circumferential thermal resistance relative to that of the fluid,

$$C = \frac{kr_0}{k_w t}. \tag{12}$$

In writing condition (11) we assume that the outside of the pipe is insulated with respect to its environment. Equation (11) constitutes the fluid temperature boundary condition at the wall. If $C \to \infty$ the wall is adiabatic and if $C = 0$ the wall is isothermal. Parameter C is identical to constant C_3 employed in Hong's paper [1].

A discussion of the boundary conditions in the horizontal z direction is necessary in order to develop an analytical solution for the velocity and the temperature. If the pipe is long and the Rayleigh number is moderate, the end effects on the velocity and temperature fields are limited to small segments of pipe near the two ends. The flow pattern throughout the middle portion of the pipe—the core region—can be regarded as fully developed, neglecting the specific conditions imposed on u, v, w at $z = 0, L/r_0$. The only condition in the z direction will be the one accounting for the temperature difference applied across the pipe. This particular point will be discussed in detail in Section 4 when we estimate the net heat leak convected from T_2 to T_1. Until then we focus on the velocity and temperature distributions in the long middle section of the pipe.

3. VELOCITY AND TEMPERATURE DISTRIBUTIONS IN THE FULLY DEVELOPED REGION

A perturbation solution in Ra as a small parameter was carried out in order to obtain analytical expressions for the velocity and temperature in the core region of the pipe. Power series expressions in Ra were assumed for u, v, w, T:

$$(u, v, w) = (u, v, w)_0 + (u, v, w)_{\mathrm{I}}Ra + (u, v, w)_{\mathrm{II}}Ra^2 + \dots \tag{13}$$

$$T = T_0 + T_{\mathrm{I}}Ra + T_{\mathrm{II}}Ra^2 + \dots. \tag{14}$$

Substituting expressions (13) and (14) into equations (1)–(3) and equating the terms containing the same power of Ra yields the necessary systems of equations for determining the functions appearing in expressions (13) and (14). Before performing the analysis, the pressure gradients appearing in the three momentum equations were eliminated by differentiating equation (2a) with respect to θ and z and equating the results with the derivatives of equations (2b) and (2c) with respect to r:

$$\frac{\partial}{\partial\theta}\left[\frac{1}{Pr}\left(u\frac{\partial u}{\partial r}+\frac{v}{r}\frac{\partial u}{\partial\theta}+w\frac{\partial u}{\partial z}-\frac{v^2}{r}\right) - \nabla^2 u + \frac{u}{r^2}+\frac{2}{r^2}\frac{\partial v}{\partial\theta}\right] - \frac{\partial}{\partial r}\left\{r\left[\frac{1}{Pr}\left(u\frac{\partial v}{\partial r}+\frac{v}{r}\frac{\partial v}{\partial\theta}+w\frac{\partial v}{\partial z}+\frac{uv}{r}\right) - \nabla^2 v + \frac{v}{r^2}-\frac{2}{r^2}\frac{\partial u}{\partial\theta}\right]\right\} = Ra\left(\sin\theta\frac{\partial T}{\partial\theta} - r\cos\theta\frac{\partial T}{\partial r}\right) \tag{15}$$

$$\frac{\partial}{\partial r}\left[\nabla^2 w - \frac{1}{Pr}\left(u\frac{\partial w}{\partial r}+\frac{v}{r}\frac{\partial w}{\partial\theta}+w\frac{\partial w}{\partial z}\right)\right] - \frac{\partial}{\partial z}\left[\nabla^2 u - \frac{u}{r^2}-\frac{2}{r^2}\frac{\partial v}{\partial\theta} - \frac{1}{Pr}\left(u\frac{\partial u}{\partial r}+\frac{v}{r}\frac{\partial u}{\partial\theta}+w\frac{\partial u}{\partial z}-\frac{v^2}{r}\right)\right] = Ra\sin\theta\frac{\partial T}{\partial z}. \tag{16}$$

(a) The zeroth order approximation of the solution to equations (1), (3), (15) and (16) is

$$(u, v, w)_0 = 0 \tag{17}$$

$$T_0 = K_1 z + K_2. \tag{18}$$

Solution (17), (18) represents the state of solid body conduction through the fluid filling the horizontal pipe of Fig. 1. Constants K_1, K_2 will later be determined from the temperature conditions prevailing in the two end regions.

(b) The first order components of u and v are

$$(u, v)_{\mathrm{I}} = 0 \tag{19}$$

while for w_{I}, T_{I} we must solve the system

$$\frac{\partial}{\partial r}(\nabla^2 w_{\mathrm{I}}) = K_1\sin\theta \tag{20}$$

$$K_1 w_{\mathrm{I}} = \nabla^2 T_{\mathrm{I}}. \tag{21}$$

Equation (20) admits a particular solution of the type

$$w_{\mathrm{I}} = K_1\sin\theta\,\psi(r) \tag{22}$$

where $\psi(r)$ satisfies the linear differential equation obtained by substituting expression (22) back into equation (20),

$$r^2\psi'' + r\psi' - \psi = r^3. \tag{23}$$

The general solution to equation (20) consists of the particular solution (22) added to the solution satisfying

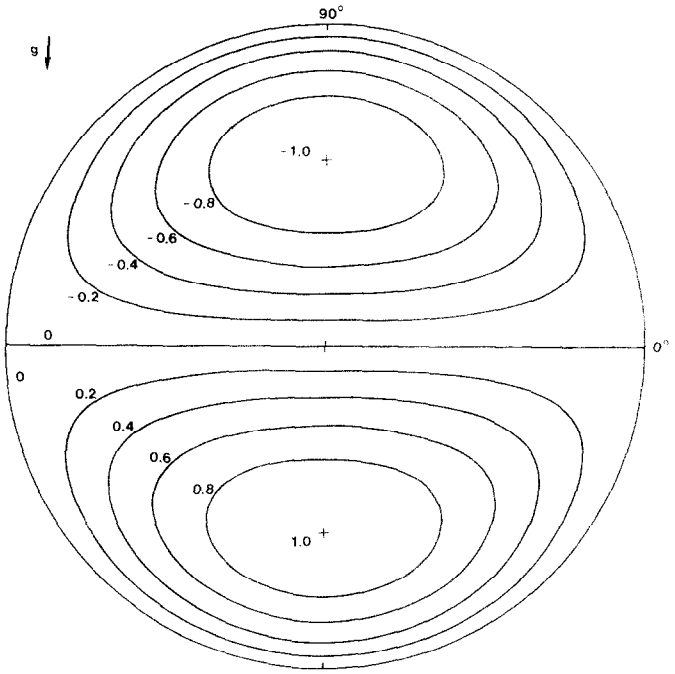

FIG. 2. Pipe cross-section showing lines of constant axial velocity (the first order velocity approximation); the numbers on the figure indicate the value of $12\sqrt{3}\, w_1/K_1$.

the homogeneous form of equation (20). Since the homogeneous solution does not depend on K_1, only the particular solution is retained based on the fact that w_1 must vanish when the pipe is infinitely long and the axial temperature gradient K_1 tends to zero. Solving equation (23) we obtain

$$\psi(r) = a_1 \frac{1}{r} + a_2 r + \frac{1}{8} r^3 \tag{24}$$

where constants a_1, a_2 are determined from the conditions that w_1 must be finite in the center of the pipe and zero around its periphery. In conclusion, the first order axial velocity component is

$$w_1 = \tfrac{1}{8} K_1 (r^3 - r) \sin\theta \tag{25}$$

which is also plotted on Fig. 2. As expected, the velocity is positive (from cold to warm) over the entire bottom half of the pipe cross-section. The maximum axial velocities occur on the vertical diameter at two points located at $r = 1/\sqrt{3}$. As shown in Fig. 2, at any of these two locations the maximum velocity is $K_1/(12\sqrt{3})$. We see also that the shape of the first order velocity distribution is independent of the temperature boundary condition at $r = 1$. Through K_1 however, the intensity of this distribution depends on the temperature boundary conditions imposed in the axial direction.

Combining the w_1 result with equation (21) leads to an equation for T_1. The solution follows a path identical to the one outlined above for w_1. Taking into consideration the temperature boundary condition at the pipe wall, equation (11), we obtain

$$T_1 = \frac{1}{192} K_1^2 \sin\theta \left(r^5 - 3r^3 + 2\frac{1+2C}{1+C} r \right). \tag{26}$$

Figure 3 shows a plot of the first order temperature variation across the pipe cross-section, for three important values of wall thermal resistance C. Overall, the pattern formed by isothermal lines is identical for both halves of the cross-section, therefore, only the top half was drawn. The lines of Fig. 3 represent lines of constant $96T_1/K_1^2$, a quantity which is always zero along the horizontal plane separating the two streams.

The first case, $C \to \infty$, is the case of counterflow in a horizontal pipe with a non-conducting wall where the heat exchange between the two streams takes place only across the horizontal interface $\theta = 0$, π. An interesting feature of this temperature pattern is that the hottest spot resides in the fluid and not at the top of the cross-section as we may have been anticipating. The top point $(1, \pi/2)$ is a saddle point at the intersection of two adiabatic surfaces, $r = 1$ and $\theta = \pi/2$. For all practical purposes, however, the region bounded by the tear-shaped isotherm of Fig. 3 ($C \to \infty$) is isothermal.

The third case, $C = 0$, shows the temperature pattern in a pipe with a highly conducting wall. This time the wall is isothermal in the θ direction. The conduction around the wall does an effective job of equalizing the temperature over the cross-section. The middle case, $C = 1$, was included to show the transition from $C \to \infty$ to $C = 0$. As the pipe wall becomes more conducting the warmest spot migrates towards the visual center of the semi-circular channel carrying the warm stream. An identical set of isothermal patterns can be constructed for the bottom half of the channel.

(c) The second order solution is obtained by collecting the Ra^2 terms resulting from substituting the series expressions (13) and (14) into the governing equations.

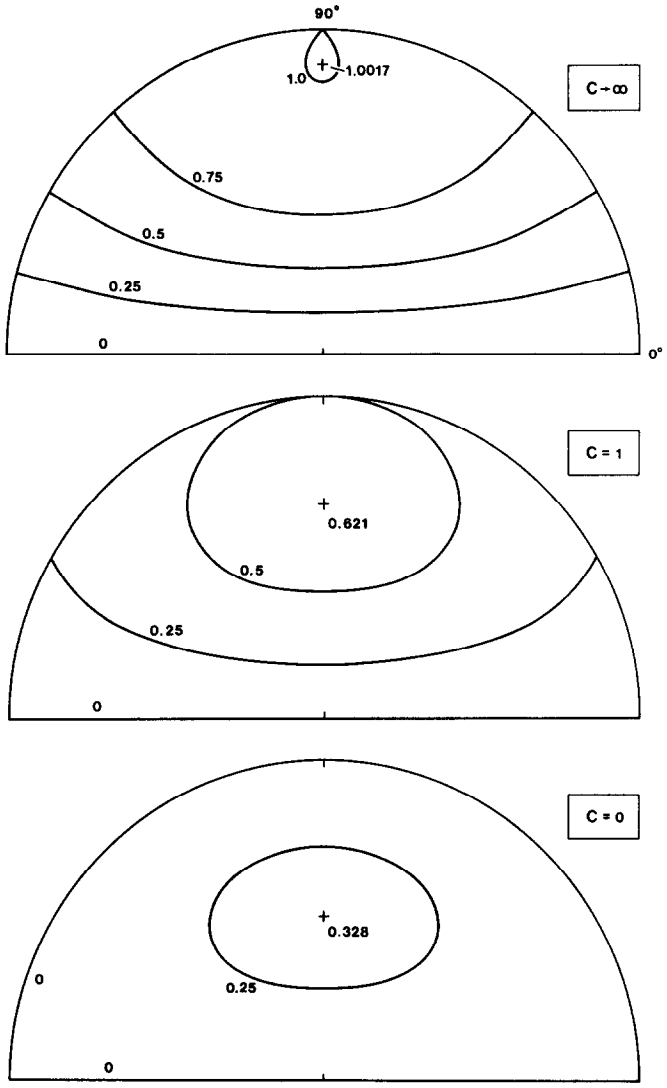

FIG. 3. Upper half of the pipe cross-section showing the first order isotherms for three different values of wall thermal resistance C; the numbers on the figure indicate the value of $96T_{\mathrm{I}}/K_1^2$.

The radial and tangential velocity components u_{II} and v_{II} are found from the system provided by equations (1) and (15), based on the method outlined for w_{I} and T_{I},

$$u_{\mathrm{II}} = \frac{K_1^2}{184\,320}\cos 2\theta(2r^7 - 15r^5 + 24r^3 - 11r) \quad (27)$$

$$v_{\mathrm{II}} = \frac{K_1^2}{184\,320}\sin 2\theta(-8r^7 + 45r^5 - 48r^3 + 11r). \quad (28)$$

From equations (16) and (3) we obtain a system for w_{II} and T_{II},

$$\frac{\partial}{\partial r}(\nabla^2 w_{\mathrm{II}}) = 0 \quad (29)$$

$$\nabla^2 T_{\mathrm{II}} = K_1 w_{\mathrm{II}}. \quad (30)$$

Using again the argument that w_{II} and T_{II} must vanish as the pipe becomes infinitely long ($K_1 \to 0$), equations (29) and (30) yield

$$(w, T)_{\mathrm{II}} = 0. \quad (31)$$

The second order velocity distribution, equations (27) and (28) represents a set of four eddies, one in each quadrant of the pipe cross-section. The streamlines of this flow pattern have been sketched on Fig. 4, where the stream function Ψ_{II} is defined as $\partial\Psi_{\mathrm{II}}/\partial\theta = -ru$, $\partial\Psi_{\mathrm{II}}/\partial r = v$. The existence of four eddies is consistent with the first order temperature distribution shown in Fig. 3: at a given height, the fluid temperature near the wall is lower than near the vertical diameter. The net effect of this second order flow pattern is additional heat transfer from the upper (warm) stream to the lower (cold) stream by natural convection.

The analytical expressions derived for the velocity and temperature fields in the horizontal pipe, equations (13) and (14), are asymptotically valid as the product RaK_1 tends to zero. When the horizontal pipe is long, the axial temperature gradient constant K_1 approaches zero. For cases in which the pipe is short, and the product RaK_1 is not sufficiently small, the perturbation analysis has to be carried beyond the second order approximation presented in this section.

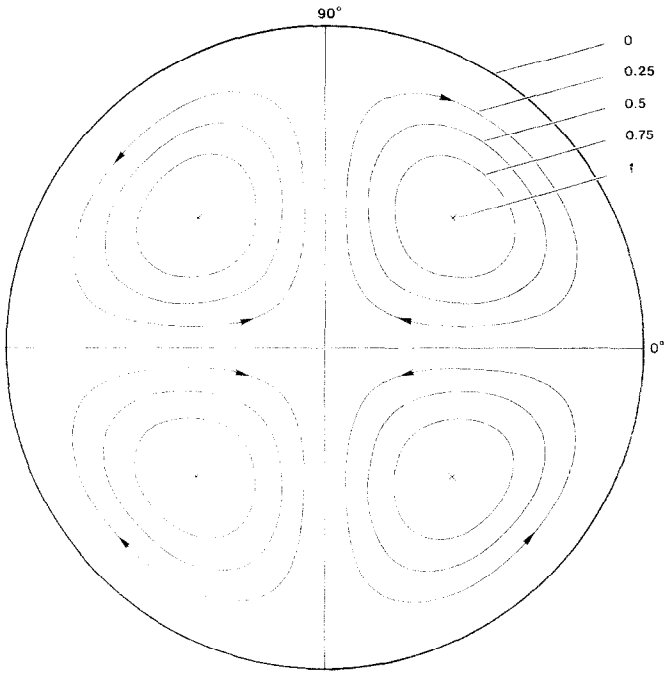

FIG. 4. Pipe cross-section showing streamlines of the second order flow pattern; the numbers on the figure indicate the value of $(2.4)\,10^5\Psi_{II}/K_1^2$.

4. THE AXIAL HEAT TRANSPORT THROUGH THE PIPE

In certain applications it is important to know the net rate of heat transfer through the pipe, from the hot end to the cold end. In liquid helium-filled channels such as in bath-cooled superconducting winding structures, a high rate of convective heat transfer is desirable in order to enhance the system's built-in capability of diffusing an accidental resistive zone (local loss of superconductivity). In other low temperature applications, horizontal fill or vent tubes connecting the cold space with a warmer environment may leak an undesirable amount of heat into the cold space via the counterflow mechanism discussed here.

The net rate of axial heat transfer Q from T_2 to T_1 through any pipe cross-section in the fully developed region is

$$\frac{Q}{\pi r_0 k(T_2-T_1)} = \frac{1}{\pi}\int_0^{2\pi}\int_0^1 \left(\frac{\partial T}{\partial z} - wT\right) r\,\mathrm{d}r\,\mathrm{d}\theta \quad (32)$$

where the LHS defines a Nusselt number for axial heat transport, Nu. Integrating the RHS using expressions (13) and (14) we obtain

$$\frac{Nu}{K_1} = 1 + \frac{2+7C}{1+C}\frac{(RaK_1)^2}{46080} + O[(RaK_1)^4] + \ldots \quad (33)$$

The third order temperature solution, T_{III}, is necessary for estimating the third term appearing in the Nusselt number expression (33); the third term will be negative accounting for the increased heat transfer between the two halves of the pipe cross-section via the eddies of Fig. 4.

Looking at the second term in expression (33) we see clearly the effect played by the wall resistance parameter C in reducing the convective heat flow through the pipe. A highly conductive wall ($C = 0$) enhances the thermal contact between the two streams and reduces the convective part to only $\frac{2}{3}$ of the convective heat leak present in exactly the same system with a non-conducting pipe wall ($C \to \infty$).

The Nusselt number Nu depends strongly on the axial temperature gradient constant K_1. The two constants K_1 and K_2 governing the velocity and temperature distributions in the core region can only be determined by taking into account the flow in the end regions. We conclude this section by presenting an approximate, asymptotically valid, estimate of the axial temperature gradient constant K_1. When the pipe is long and the Rayleigh number is moderate, experience with parallel-plate horizontal channels shows that the core regime, equations (13) and (14), fills almost the entire length of the pipe [2–6]. Under these circumstances, the relative temperature difference between streams at any z is much smaller than the ΔT applied across the ends of the pipe. The bulk temperature at $z = 0$ is close to T_1 while at $z = L/r_0$ it is approaching T_2. These conditions are sufficient for determining the unknown constants. The result is

$$K_1 \cong r_0/L, \qquad K_2 \cong 0. \quad (34)$$

Approximation (34) is valid as $r_0/L \to 0$. For constant r_0/L and increasing Ra, K_1 decreases gradually on account of the widening temperature difference between streams. The function describing the dependence of K_1, K_2 on Ra and r_0/L can be derived by applying the end-integral technique used by Bejan and Tien for parallel-plate channels [6]. According to this procedure, the momentum and energy equations are first integrated over the two end regions in which the

fully-developed (core) solution is not valid. Velocity and temperature profiles which match the core solution at the imaginary transition between the core region and the end region are then substituted into the two integral conditions. For each end, the integral procedure yields a single implicit function relating K_1, K_2, Ra and r_0/L. As shown by Bejan and Tien [6], the end-integral technique can be applied to closed ends as well as open ends (when the pipe communicates freely with a large reservoir).

5. THE WALL TEMPERATURE

The temperature distribution in the pipe wall is relevant to estimating the thermal stresses induced by the natural counterflow. This result follows immediately from the temperature field derived in Section 3, equation (14),

$$T(1,\theta,z) = K_1 z + K_2 + \frac{K_1^2 Ra}{96}\frac{C}{1+C}\sin\theta + \ldots \quad (35)$$

showing that the maximum circumferential temperature gradient occurs at $\theta = 0, \pi$. The dependence of $\partial T/\partial\theta$ on C is of special interest. Keeping everything else constant, a non-conducting wall ($C \to \infty$) experiences the maximum gradient possible. In a perfectly conducting wall ($C = 0$) the temperature is the same over the entire circumference and the gradient is zero. The intermediate case $C = 1$ is one in which the circumferential gradient at $\theta = 0, \pi$ is exactly half of the maximum present in a non-conducting wall. This conclusion can also be drawn from Fig. 3.

6. DISCUSSION

The wall temperature distribution derived analytically in the preceding section can now be compared with the numerical result published recently by Hong [1]. To begin with, Hong's numerical solution is based on the assumption of neither radial nor tangential motion in the fluid. Thus, Hong's numerical solution for w and T is equivalent to only the first order solution developed in Section 3. In Fig. 2 of his work, Hong plotted the computed wall temperature as a function of θ, for five different values of wall thermal resistance. The lowest value used was $C = 0.1$ and the highest $C = 10$. For a direct comparison, the dimensionless wall temperature difference function ϕ employed by Hong corresponds to the first order wall temperature distribution, i.e. the third term of expression (35). In terms of our notation and based on expression (35), Hong's function ϕ becomes

$$\phi = \frac{5\pi}{32}\frac{C}{1+C}\sin\theta. \quad (36)$$

Comparing the analytical result (36) with the computed $\phi(\theta)$ as reported by Hong [1], we find a disagreement which becomes more pronounced as C increases. Specifically, if $C = 0.1$, the maximum temperature gradient plotted by Hong in his Fig. 2 is 4.1 times smaller than the gradient calculated using equation (36). For $C = 10$, the gradient reported by Hong is 32 times smaller than the analytical result. Hong's plot shows in effect that the temperature distribution in a highly conducting wall, $C = 0.1$, is almost the same as the distribution in a highly non-conducting wall, $C = 10$. This discrepancy appears to be due to the fact that, unlike the present analysis, Hong's numerical solution relies on the assumption that a thin solid sheet placed at $\theta = 0, \pi$ separates the two streams of the counterflow. In other words, the natural convection counterflow was approximated by forced convection in two adjacent channels with semi-circular cross-sections and prescribed axial pressure gradients.

7. CONCLUSION

In order to understand the mechanism of axial heat transfer through a long insulated horizontal pipe exposed to an end-to-end temperature difference the fully-developed natural convection in the middle portion of the pipe was studied analytically. In Section 3 we presented an asymptotic solution for the velocity and temperature distribution in the pipe cross-section, valid for small and moderate values of the product RaK_1. The Nusselt number for axial heat-transfer Nu calculated in Section 4 was shown to depend on the Rayleigh number Ra and on the aspect ratio L/r_0. The pipe wall thermal conductance can substantially decrease the net rate of axial heat transfer through the horizontal pipe. The circumferential temperature distribution induced in the pipe wall by the natural counterflow of Fig. 1 was derived analytically in Section 5. The maximum circumferential temperature gradient based on this analysis was shown to be considerably larger than the maximum gradient suggested by a published numerical analysis [1].

Acknowledgement—A. Bejan acknowledges the support received from the Miller Institute for Basic Research in Science, University of California, Berkeley, in the form of a postdoctoral research fellowship.

REFERENCES

1. S. W. Hong, Natural circulation in horizontal pipes, *Int. J. Heat Mass Transfer* **20**, 685–691 (1977).
2. D. E. Cormack, L. G. Leal and J. Imberger, Natural convection in a shallow cavity with differentially heated end walls. Part 1. Asymptotic theory, *J. Fluid Mech.* **65**, 209 (1974).
3. D. E. Cormack, L. G. Leal and J. H. Seinfeld, Natural convection in a shallow cavity with differentially heated end walls. Part 2. Numerical solutions, *J. Fluid Mech.* **65**, 231 (1974).
4. J. Imberger, Natural convection in a shallow cavity with differentially heated end walls. Part 3. Experimental results, *J. Fluid Mech.* **65**, 247 (1974).
5. D. E. Cormack, G. P. Stone and L. G. Leal, The effect of upper surface conditions on convection in a shallow cavity with differentially heated end-walls, *Int. J. Heat Mass Transfer* **18**, 635 (1975).
6. A. Bejan and C. L. Tien, Laminar natural convection in horizontal channels with different end temperatures—an approximate solution. To be published.
7. S. Foner and B. B. Schwartz, *Superconducting Machines and Devices*. Plenum, New York (1974).

ECOULEMENT NATUREL DEVELOPPE A CONTRE-COURANT DANS UN TUBE HORIZONTAL AVEC DIFFERENTES TEMPERATURES AUX EXTREMITES

Résumé—La différence de température appliquée aux extrémités d'un tube horizontal provoque un écoulement naturel à contre-courant dans lequel le fluide froid s'écoule au fond du tube vers l'extrémité chaude tandis qu'un écoulement chaud s'opère au dessus et dans la direction opposée. L'article présente une solution asymptotique pour les distributions de vitesse et de température dans la portion centrale du tube avec des parois conductrices. L'influence de la conduction circonférentielle, dans l'épaisseur du tube, sur la distribution de température analytique donne le transfert axial net par la convection à contre-courant. On compare les résultats obtenus pour la distribution de température dans la paroi du tube avec des résultats numériques récemment publiés.

VOLLSTÄNDIG AUSGEBILDETE FREIE GEGENSTRÖMUNG IN EINEM LANGEN HORIZONTALEN ROHR MIT UNTERSCHIEDLICHEN ENDTEMPERATUREN

Zusammenfassung—Die Temperaturdifferenz zwischen zwei gegenüberliegenden Enden eines horizontalen Kanals erzeugt eine natürliche Gegenströmung, in welcher kälteres Fluid entlang des Kanalbodens zum warmen Ende fließt, während eine warme Strömung in entgegengesetzter Richtung entlang Kanaloberseite fließt. Diese Veröffentlichung zeigt eine asymptotische Lösung für die Geschwindigkeits- und Temperaturverteilung im mittleren Teil eines langen horizontalen Rohres mit leitenden Wänden. Der Einfluß radialer Wärmeleitung in der Rohrwand auf die Temperaturverteilung im Fluid wird untersucht. Eine analytische Form wird für rein axialen Wärmestrom bei gegeneinander strömender freier Konvektion erreicht. Die dargestellten Ergebnisse für die Temperaturverteilung in der Rohrwand werden mit numerischen Lösungen verglichen, die kürzlich veröffentlicht wurden.

УСТАНОВИВШЕЕСЯ СВОБОДНОКОНВЕКТИВНОЕ ПРОТИВОТОЧНОЕ ТЕЧЕНИЕ В ДЛИННОЙ ГОРИЗОНТАЛЬНОЙ ТРУБЕ С РАЗНЫМИ ТЕМПЕРАТУРАМИ НА КОНЦАХ

Аннотация — Разность температур на концах горизонтальной трубы создает свободноконвективное противоточное течение жидкости в трубе: более холодная жидкость течет в нижней части трубы и направлена в сторону с более высокой температурой, в то время как теплая движется в верхней части трубы в противоположном направлении. Найдено асимптотическое решение для профилей скорости и температуры в средней части длинной горизонтальной трубы с теплопроводящей стенкой. Исследуется влияние передачи тепла теплопроводностью в стенке по периметру трубы на распределение температуры в жидкости. Получено аналитическое выражение для результирующего аксиального переноса тепла противоточной естественной конвекцией. Данные по распределению температуры в стенке трубы сравниваются с опубликованными ранее численными результатами.